CHAPTER IV

PREPARATION AND CHARACTERIZATION OF CELLULOSE WHISKER-REINFORCED SILK FIBROIN SPONGE FOR YEAST IMMOBILIZATION FOR ETHANOL PRODUCTION

4.1 Abstract

A bionanocomposite sponge consisting of silk fibroin (SF) and cellulose whiskers (CLWs) was developed for yeast cell immobilization for ethanol production. Silk fibroin, a protein in silk fibers produced by the mulberry silkworm (*Bombyx mori*), was used as a matrix in the bionanocomposite sponges. Cellulose whiskers having an aspect ratio of 80 were used as reinforcement. The bionanocomposite sponges having SF/CLWs weight ratios of 100/0, 90/10, 80/20, 70/30, 60/40 and 50/50 were fabricated by using a freeze-drying technique, followed by immersion in an aqueous methanol solution in order to induce conformation transition of silk fibroin to be the beta-sheet structure, an water-insoluble form. Fourier transform infrared spectrophotometry (FTIR) spectra showed beta-sheet conformation of SF after the methanol treatment for the studied SF/CLWs weight ratios. The presence of CLWs in the bionanocomposite sponges not only enhanced the conformation transition of SF but also increased the compression modulus as well as reduced the shrinkage of the bionanocomposite sponges. The formation of beta-sheet structure of SF significantly increased water stability of the bionanocomposite sponges. The field emission scanning electron micrographs showed that the bionanocomposite sponges exhibited an interconnected porous structure, providing high surface area for immobilizing *Saccharomyces cerevisiae burgundy* KY11 yeast cells. The sponge with the SF/CLWs weight ratio of 50/50 showed the highest average number of yeast cell attachment at 3.1×10^{10} cells/g sponge.

Keyword: Silk fibroin/Cellulose whiskers/Yeast immobilization/ethanol

4.2 Introduction

Nowadays, petroleum oil is depleted faster because of the continuous overconsumption of the reserved oil. Therefore, there are several attempts to search for alternative energy sources. Among a variety of potential candidates, bioethanol is in great interest. Cell immobilization is a technique involving the attachment of yeast cells to the polymeric matrices via physical attachment, covalent bonding, or cell entrapment. Cell immobilization is able to eliminate the inhibition caused by a high concentration of substrate or product which normally found during the fermentation process and, as a consequence, the enhanced ethanol yield can be obtained.

SF is a protein in silk fibers obtained from the cocoons of the mulberry silkworm *Bombyx mori*. SF has been reported to be useful in biomedical applications due to its good biocompatibility as well as biodegradability and high cytocompatibility. Nevertheless, the post treatment, such as methanol treatment, is usually required to convert the random coil conformation to the beta-sheet structure which is a water-stable conformation. However, methanol treatment causes the shrinkage and the reduction of their dimensional stability.

CLWs extracted from banana rachis were used as reinforcement in the bionanocomposite sponges to achieve structural integrity of SF based sponges during fermentation process. The bionanocomposite sponges consisting of SF and CLWs were prepared by freeze drying technique. The effect of the blended ratios on the chemical structure and morphology of the bionanocomposite sponges was investigated. The potential use of the bionanocomposite sponges as a supporting material used in cell immobilization for ethanol production was evaluated.

4.3 Experimental

4.3.1 Materials

4.3.1.1 Silk Cocoons and Banana Rachises

The *Bombyx mori* silkworm cocoons were obtained from the Queen Sirikit Department of Sericulture (Thailand).The *Musa sapientum Linn* banana rachises were purchased from local banana farm in Ratchaburi province, Thailand.

4.3.1.2 Yeast Cells

Saccharomyces cerevisiae burgundy KY11 was purchased from Institute of Food Research and Product Development, Kasetsart University in the form of fresh cell culture.

4.3.1.3 Other Chemicals

Methanol (CH_3OH) and ethanol (C_2H_5OH) (99.5 % purity), analytical grade, were purchased from RCI Labscan., Ltd. Analytical grade calcium chloride dihydrate ($CaCl_2\,2H_2O$) was purchased from Analar®. Sodium hydroxide (NaOH) and sodium carbonate (Na_2CO_3) pellets, analytical grade, were purchased from RANKEM. Hydrogen peroxide (H_2O_2) was purchased from Fisher Scientific Co., Ltd D-glucose anhydrous, bacteriogical peptone, and yeast extract powder were purchased from UNIVAR, CONDA, and HimediA, respectively. Sodium potassiam tartrate ($KNaC_4H_4O_6 \cdot 4H_2O$) and 3,5- dinitrosalicylic acid (DNS) were purchased from Sigma Aldrich.

4.3.2 Equipments

Fourier transformed infrared (FTIR) spectroscopy, A Thermo Nicolet Nexus 671 FTIR) spectrophotometer was used to characterize the chemical structure and conformation of SF, CLWs, and bionanocomposite sponges. The spectra were collected at a resolution of 4 cm^{-1} and 64 scans in the wavenumber range of 4000 cm^{-1} to 400 cm^{-1}. A HITACHI S4800 FE-SEM microscope was used to observed both surface and cross-section morphology of the sponges at an operating voltage of 2 kV. The specimens

were coated with platinum by using a sputtering equipment operated for 200 seconds before the SEM observation. Transmission electron microscopy (TEM) image of cellulose whiskers were taken by a JEOL JEM 2100 TEM microscope at an operating voltage of 200 kV. Samples for TEM observation were prepared by stainning the diluted cellulose whiskers suspension with 1 % uranyl acetate aqueous solution. The sample was dropped on a carbon-coated copper grid and air-dried. To evaluate the compression modulus, the compression test was performed by using Lloyd instrument at crosshead speed 1 mm/minute at room temperature. The compressive modulus was calculated from the initial slope of the linear portion of the stress–strain curve. The sample number was five for each experimental group. Sampling the suspension of ferment at 0, 8, 16, 24, 36 and 48 hours then centrifuged at 10000 rpm 4°C for 10 minutes in order to separate the cell pellets out of the supernatant. An Tecant Infinite® 200 PRO UV-vis spectrophotometer was used to examine the utilization of reducing sugar by yeast cells during fermentation process. To determine the immobilization efficiency, the utilization of reducing sugar during fermentation process was evaluated by using the DNS method (Miller, 1959) based on the precipitation of residual sugar. The color intensities in terms of absorbance were measured at a wavelength of 546 nm. The sugar concentration was then determined from the glucose standard curve prepared in the concentration range of 1% to 100% (w/v). The bioethanol concentration was determined by using a Shimazu GC-7AG instrument equipped with a flame ionization (FID) detector. A steel gas chromatograph column packed with Porapak Q was used. The cell pellets were resuspended in a 0.85 % NaCl solution before dropped to a Neubaeur Precicolor HBG heamacytometer counting chamber. The number of yeast cells was counted directly under an Olympus CX31 OM microscope in order to evaluate the cell growth during fermentation process.

4.3.3 Methodology

4.3.3.1   Preparation of Silk Fibroin Solution (SF)

B. *mori* silk cocoons were cut into small pieces, washed with water, and dried at 40 °C overnight. The silk degumming process was carried out by boiling the silk cocoons in a 0.05 % (w/v) Na_2CO_3 solution for 15 minutes (repeated for 2 times). The degummed silk was dried in an oven at 40 °C overnight before being dissolved in a polar solvent system containing $CaCl_2$:ethanol:water molar ratio of 1:2:8. The resulting fibroin solution was dialyzed against distilled water until negative test of $AgNO_3$ was obtained, followed by centrifugation at 10,000 rpm for 10 minutes. The as-prepared SF solution was kept at 4 °C until use.

4.3.3.2   Preparation of Cellulose Whiskers (CLWs)

M. *sapientum Linn* banana rachis was cut into the length of 100 mm to 300 mm and dried overnight in an oven at 40 °C. Dried banana rachises were then soaked in a 2 %(w/v) NaOH solution at 80 °C for 2 hours. After thoroughly rinsed with distilled water, the rachises were treated with a 3 % (w/v) H_2O_2 solution at 70 °C for 2 hours. The purified cellulose was hydrolyzed at 60 °C for 4 hours in a 65% (w/v) sulfuric acid solution. The resulting CLWs were diluted with distilled water and centrifuged at 10,000 rpm for 10 min. After the centrifugation, the CLWs suspension was neutralization by dialyzed against distilled water until neutral pH.

4.3.3.3   Preparation of Bionanocomposite Sponges

The as-prepared SF solution was diluted with distilled water to achieve a desired concentration at 3% (w/v). The CLWs suspension was ultrasonicated for 15 minutes prior to adding into the SF solution at five different CLWs content — 10 %, 20 %, 30%, 40% and 50% based on weight of final solution — with slow mechanical stirring. The mixture was stirred for 10 minutes and 1 ml of the well-mixed solution was pipetted to each well of COSTAR® 24-multi-wells culture plate and freeze dried at -40°C overnight.

4.3.3.4 Methanol Treatment of Bionanocomposite Sponges

The SF sponges both with and without CLWs were immersed in a 90% (v/v) methanol solution for 10 minutes. After that the methanol-treated sponges were washed with an excessive amount of distilled water and dried by using a freeze dryer at -40 °C for 24 hours.

4.3.3.5 Inoculums Preparation

To prepare an inoculum, 2 ml of the diluted yeast suspension was added in a cotton-plugged 100 ml Erlenmeyer flask containing 18 ml of Yeast peptone dextrose (YPD) broth growth medium consisting of glucose, peptone, and yeast extract at a concentration of 20 $g \cdot l^{-1}$, 20 $g \cdot l^{-1}$, and 10 $g \cdot l^{-1}$, respectively. The yeast culture was incubated in a shaking at 150 rpm and 30 °C for 24 hours in order to get mature yeast cell with a cell concentration more than 10^8 $cells \cdot ml^{-1}$ for being used in the cell immobilization step.

4.3.3.6 Cell Immobilization

The methanol-treated bionanocomposite sponges and 250 mL of YPD broth were autoclaved separately at 121°C for 15 minutes. The inoculum cell suspension together with the methanol-treated bionanocomposite sponges were then added to the sterilized medium. To induce natural cell adhesion, the sponges were immersed in the culture medium and then incubated in a shaking incubator at 150 rpm and 30°C for 48 hours following by freeze drying.

4.3.3.7 Vitalization of Yeast Cell Immobilized in Bionanocomposite Sponges

Immobilized cells of *Saccharomyces cerevisiae* burgundy KY11 in bionanocomposite sponges was revitalized in a 250 ml Erlenmeyer flask containing 100 ml of YPD nutrient medium in a shaking incubator at 150 rpm and 30° C for 24 hour.

4.3.3.8 Batch Fermentation

Batch fermentation with varied glucose solution concentration, 10%, 20%, 30% and 40% (w/w), of both suspended cells (used as control) and

immobilized cells of *Saccharomyces cerevisiae* burgundy KY11 in bionanocomposite sponges were used in an equivalent number of yeast cells. Suspended cell and immobilized cell were transferred to a cotton plugged 250 ml Erlenmeyer flask containing 100 ml of glucose solution. The culture medium was sampled at a specific time interval for 48 hours and was then centrifuged at 10,000 rpm for 10 minutes to remove cell pellets. The clear supernatant was further subjected the reducing sugar concentration, ethanol content, and cell viability analyses by DNS method, Gas chromatography (GC) and direct counting using Neubaeur Precicolor HBG heamacytometer counting chamber, respectively.

4.3.3.9 Repeat Batch Fermentation

The 50/50 weight ratio of SF/CLWs bionanocomposite sponges were applied into a 100 ml of growth medium consisting of glucose, peptone, and yeast extract at a concentration of 400 $g \cdot l^{-1}$, 20 $g \cdot l^{-1}$, and 10 $g \cdot l^{-1}$, respectively, which used as a substrate. The flasks were shaken in the incubator at 150 rpm at 30°C. The duration of each batch was set at 48 hours. After that, the bionanocomposite sponges were transferred into the new freshly culture medium. The culture was sampling at a specific time interval and was further investigated the reducing sugar residue, ethanol content and amount of yeast cell.

4.3.4 Analytical Methods and Measurements

4.3.4.1 Fourier Transformed Infrared (FTIR) Spectroscopy

A Thermo Nicolet Nexus 671 FTIR spectrophotometer was used to characterize the chemical structure and conformation of SF, CLWs, and CLWs-reinforced SF sponges. The spectra were collected at a resolution of 4 cm^{-1} and 64 scans in the wavenumber range of 4000 cm^{-1} to 400 cm^{-1}.

4.3.4.2 Field Emission Scanning Electron Microscopy (FE-SEM)

A HITACHI S4800 FE-SEM microscope was used to observe both surface and cross-section morphology of the CLWs-reinforced SF sponges at an operating voltage of 2 kV. The specimens were coated with platinum by using a sputtering equipment operated for 200 seconds before the SEM observation.

4.3.4.3 Transmission Electron Microscopy (TEM)

The TEM image of cellulose whiskers were taken by a JEOL JEM 2100 TEM microscope at an operating voltage of 200 kV. Samples for TEM observation were prepared by staining the diluted cellulose whiskers suspension with 1 % uranyl acetate aqueous solution. The sample was dropped on a carbon-coated copper grid and air-dried.

4.3.4.4 Shrinkage of Bionanocomposite Sponges

The volume of the bionanocomposite sponges before and after methanol treatment was investigated to calculate the shrinkage (%) after treated with methanol.

$$\text{Shrinkage (\%)} = \frac{(V_i - V_f)}{V_i} \times 100$$

V_i : the volume of the sponges before methanol treatment

V_f : the volume of the sponges after methanol treatment

4.3.4.5 Lloyd Instrumental

To evaluate the compression modulus, the compression test was performed at crosshead speed 1 mm/minute at room temperature. The compressive modulus was calculated from the initial slope of the linear portion of the stress–strain curve. The sample number was five for each experimental group.

4.3.4.6 Weight Loss of Bionancomposite Sponges

To identify the stability of bionanocomposite sponge in water, both non-methanol treated and methanol treated bionanocomposite sponges were immersed in distilled water and incubated at 30°C 150 rpm for 72 hours. Weight loss was calculated from this equation;

$$\% \text{ weight loss} = \frac{(W_i - W_f)}{W_i} \times 100$$

W_i : initial dry weight of bionanocomposite sponge

W_f : final dry weight of bionanocomposite sponge

4.3.4.7 *Ultraviolet-Visible (UV-vis) Spectroscopy*

An Tecant Infinite® 200 PRO UV-Vis spectrophotometer was used to examine the utilization of reducing sugar by yeast cells during fermentation process. To determine the immobilization efficiency, the utilization of reducing sugar during fermentation process was evaluated by using the DNS method (Miller, 1959) based on the precipitation of residual sugar. The tests were made with 3 ml of DNS reagent added to 3 ml of sample solution. The color intensities in terms of absorbance were measured at a wavelength of 575 nm. The sugar concentration was then determined from the glucose standard curve prepared in the concentration range of 0.1 mg/ml to 1 mg/ml. The sugar consumption was calculated by this equation:

$$Sugar\ consumption = S_0 - S$$

S = glucose concentration (g/l) at 48 hour fermentation time

S_0 = glucose concentration (g/l) at 0 hour fermentation time

4.3.4.8 *Gas Chromatography (GC)*

The bioethanol concentration was determined by using a Shimazu GC-7AG instrument equipped with a flame ionization (FID) detector. A steel gas chromatograph column packed with Porapak Q was used. Temperature of the column and injector were fixed constant at 170 °C and 220 °C, respectively. Nitrogen (N_2) gas with the flow rate of 45 ml min^{-1} was used as a carrier gas. Peak areas in the GC chromatograms were compared with ethanol with known concentration of 0.01% to 20% (v/v) in order to calculate bioethanol concentration in the test sample. Ethanol production was calculated by this equation:

$$\text{Ethanol production} = P - P_0$$

P = ethanol concentration (g/l) at 48 hour fermentation time

P_0 = ethanol concentration (g/l) at 0 hour fermentation time = 0

4.3.4.9 Optical Microscopy (OM)

Sampling the suspension of ferment then centrifuged at 10000 rpm 4°C for 10 minutes in order to separate the cell pellets out of the supernatant. The cell pellets were resuspended in a 0.85 % NaCl solution before dropped to a Neubaeur Precicolor HBG heamacytometer counting chamber. The number of yeast cells was counted directly under an Olympus CX31 OM microscope in order to evaluate the cell growth during fermentation process, immobilization efficiency according to this equation:

$$\text{Immobilization efficiency (\%)} = \frac{(X_i)}{(X_i + X_f)}$$

X_i = immobilized cell concentration in sponges (cell/ml)

X_f = free cell concentration in medium

$X_t = X_i + X_f$

4.4 Results and Discussion

4.4.1 Production Yield of SF Solution

The production yield of SF solution obtained from 10 g of degummed silk. The 120 ml of as-prepared silk fibroin solution had weight content about 5.8% (w/v) as shown in Table 4.1

Table 4.1 Production yield of silk fibroin solution.

Material	Dry weight (g)
Degummed silk	100
Silk fibroin	87

4.4.2 Characterization of SF Solution

The structure of SF was examined by FT-IR as shown in Figure 4.1. The FTIR characteristic peaks of SF film located at 1654 cm^{-1} (amide I) and 1542 cm^{-1} (amide II) which are attributed to a random coil structure (Yang *et al.,* 2000; Noshiki *et al.,* 2002; Freddi *et al.,* 2003; Park *et al.,* 2004). SF is natural biopolymer which exists in several conformations such as random coil and beta-sheet structure. To prepare SF-based material, SF must be dissolve in the proper solvent in order to disrupt the intermolecular hydrogen bond of beta -sheet structure. The SF solution is called "regenerated SF" which posses random coil structure. However, before being used, the regenerated SF was induced its beta-sheet structure. In this experiment, methanol treatment was used to change the SF conformation.
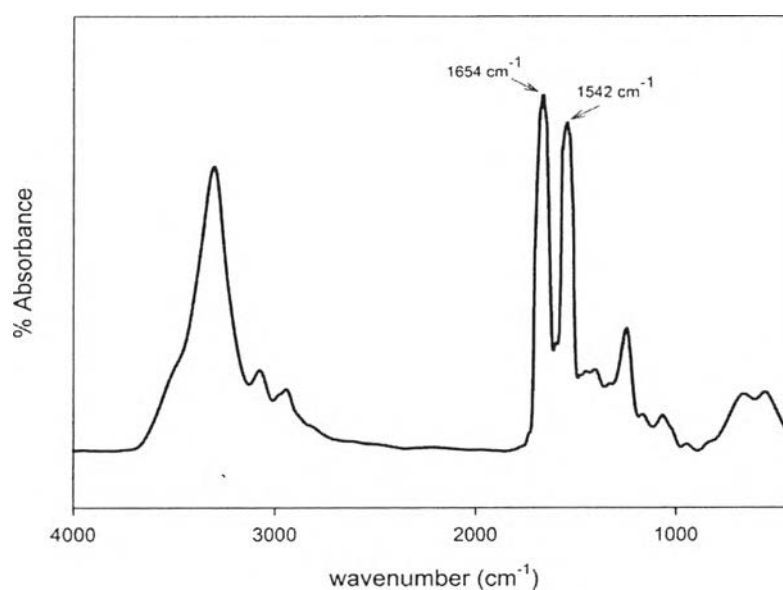
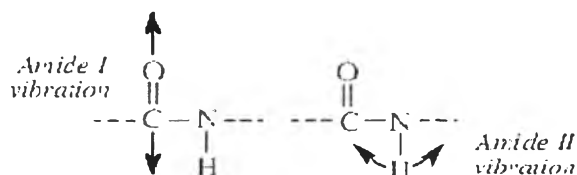**Figure 4.1** FTIR spectra of SF solution.

Figure 4.2 Characteristic peaks of silk fibroin.

4.4.3 Production Yield of CLWs Suspension

The production yield of CLWs suspension after acid hydrolysis of 100 g banana rachis was 1.3% (w/v) of CLWs suspension 122 ml as shown in Table 4.2

Table 4.2 Production yield of CLWs suspension.

Process	Dry weight (g)
Banana rachis	100
After Immersed in NaOH	43.19
After bleaching step	35.12
After acid hydrolysis	22.65

4.4.4 Characterization of CLWs Derived from Banana Rachis

4.4.4.1 Morphology Analysis of CLWs

TEM was used to observe the morphology of CLWs. The CLWs extracted from banana rachis exhibited long and slender nanofibril structure with the length (L) and diameter (D) in the range of 0.92 μm to 4.20 μm and 10 nm to 69 nm, respectively. The average length and diameter of the CLWs were found to be 2.18 μm and 27 nm, respectively, corresponding to the aspect ratio (L/D) of about 80 as shown in figure 4.3.
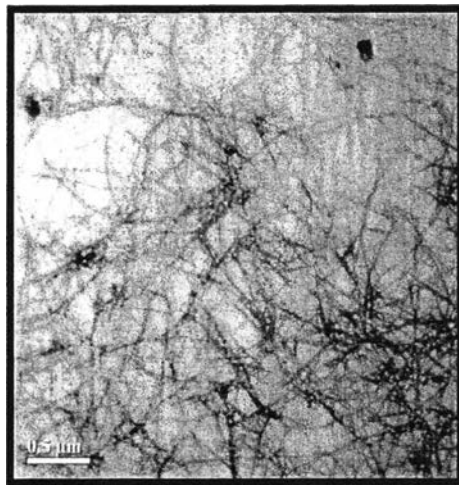
Figure 4.3 TEM image of CLWs obtained from acid hydrolysis of banana rachis.

4.4.4.2 Chemical Analysis of CLWs

The chemical structure of cellulose whiskers (CLWs) from banana rachis was investigated with the use of the FTIR spectroscopy was shown in Figure 4.4. The characteristic peaks was shown in table 4.3. Compared with Bacterial cellulose (BC), the biosynthesis cellulose from *Acetobacter xylinum* which have no hemicelluloses and lignin, CLWs and BC showed almost the same dominated characteristic peaks. The peak at 1060 cm^{-1} is assigned to C-O stretching vibration of cellulose. The asymmetric C-O-C of glycosidic ring was appeared at 1160 cm^{-1}.The peaks at 1320 cm^{-1} and 1426 cm^{-1} were corresponding to stretching of CH_2 in cellulose. However, the CLWs still contained some small amount lignin due to the peak at 1632 which corresponding to C=C in benzene ring was appeared. However, Sun *et al.* (2004) claimed that bleaching by sodium chlorite was more effectively removed lignin than using hydrogen peroxide.

Table 4.3 The main functional group of CLWs and BC.

Wavenumber (cm^{-1})	Assignment	Origin
1632	C=C	lignin
1426, 1320	streching C-H$_2$	cellulose
1160	asymmetric C-O-C	glycosidic ring
1060	streching C-O	cellulose
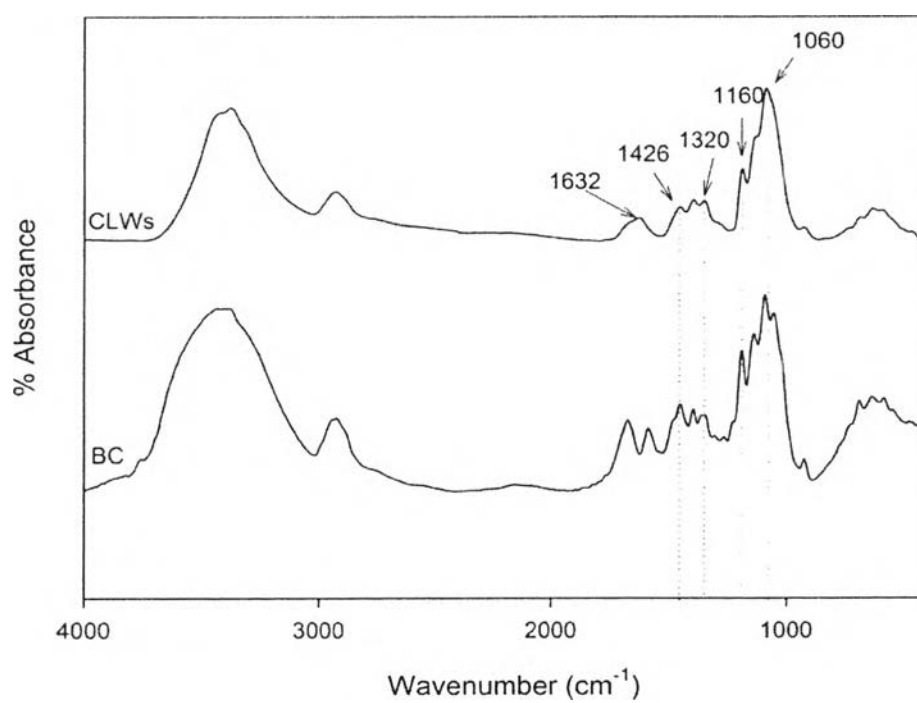
Figure 4.4 FTIR spectra of native cellulose (banana rachis) and CLWs.

4.4.5 Characterization of Bionanocomposite Sponges

4.4.5.1 Morphological Analysis of Bionanocomposite Sponges

The morphological of bionanocomposite sponges were shown in Figure 4.5 and 4.6. The surface of SF, CLWs, and SF/CLWs composites sponges exhibited porous structure. These interconnected pores allowed the substrate to pass through the materials to the yeast cells attached inside the porous sponges during a fermentation process as well as for nutrient and waste transport. The structure of the bionanocomposite sponges is controlled by the freezing temperature and solid concentration of polymer solution. The initial ice crystals are nucleated at the bottom of SF/CLWs mixture and elongated to the top surface. The pore structure of the sponges mirrors the ice-crystal morphology after freezing. The slower freezing rate generates larger ice crystal, thus the larger pores remained after sublimation step. The presence of CLWs in the SF sponges resulted in the larger mean pore width. This might be explained that the rod-like crystalline structure of CLWs may obstruct the direction and speed of heat transfer of water molecule, causing slow *in situ* freezing rate, enlarging the ice particles, and finally resulting in the larger pore width (Shapiro and Cohen, 1996).

Table 4.4 Average pore size of bionanocomposite sponges

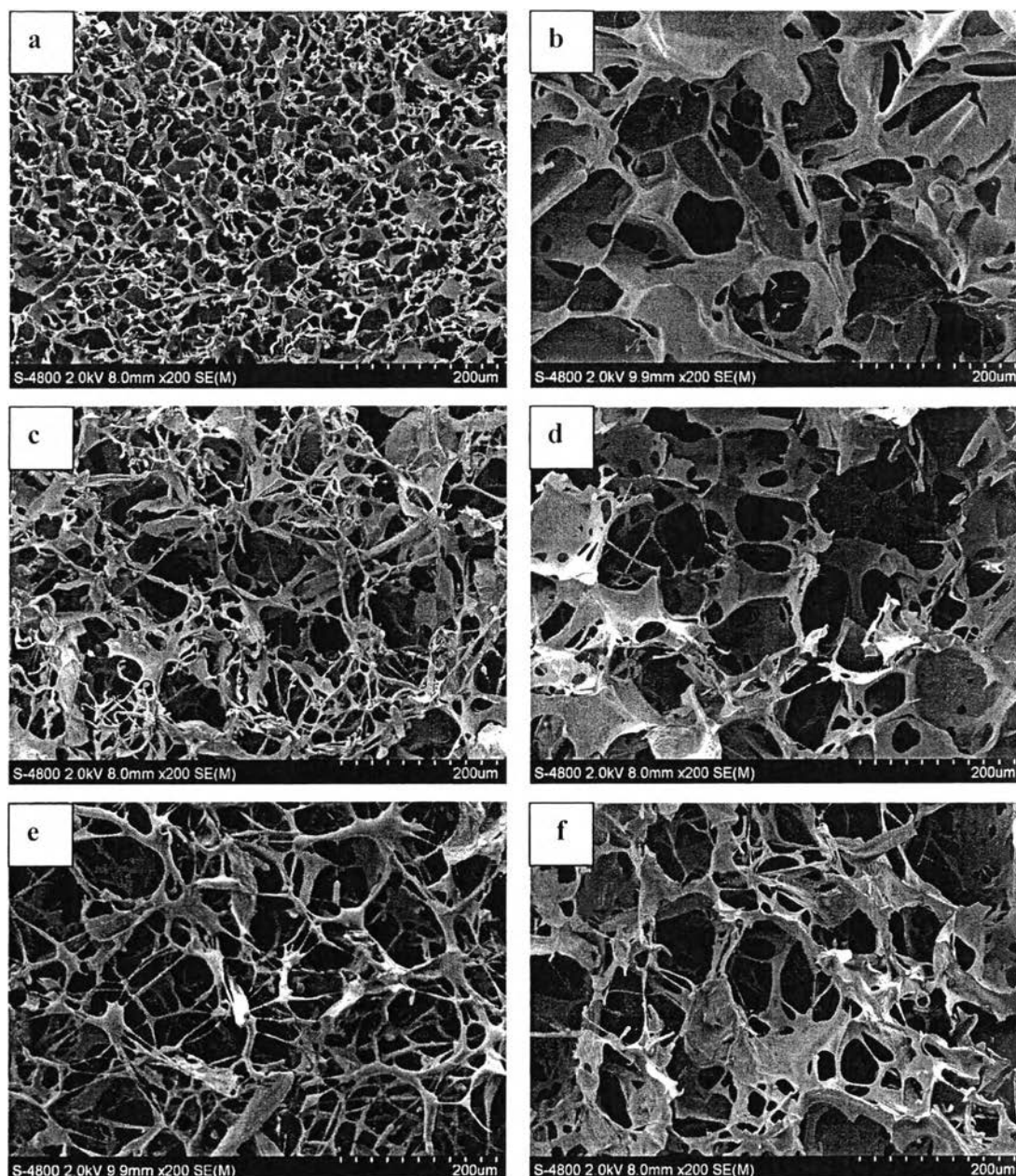| Weight ratio of SF/CLWs bionanocomposite sponges	Average pore width (μm)
100:0	21.7 ± 9.6
90:10	45.4 ± 15.5
80:20	47.1 ± 20.9
70:30	48.6 ± 28.1
60:40	53.8 ± 25.0
50:50	59.3 ± 18.7

Figure 4.5 SEM images of top surface of (a) SF sponge, (c) and (e) bionanocomposite sponges at SF/CLWs ratio of 90/10 and 80/20 respectively. (b), (c) and (f) represented cross sectional part of SF sponge, bionanocomposite sponges at SF/CLWs ratio of 90/10 and 80/20 respectively.
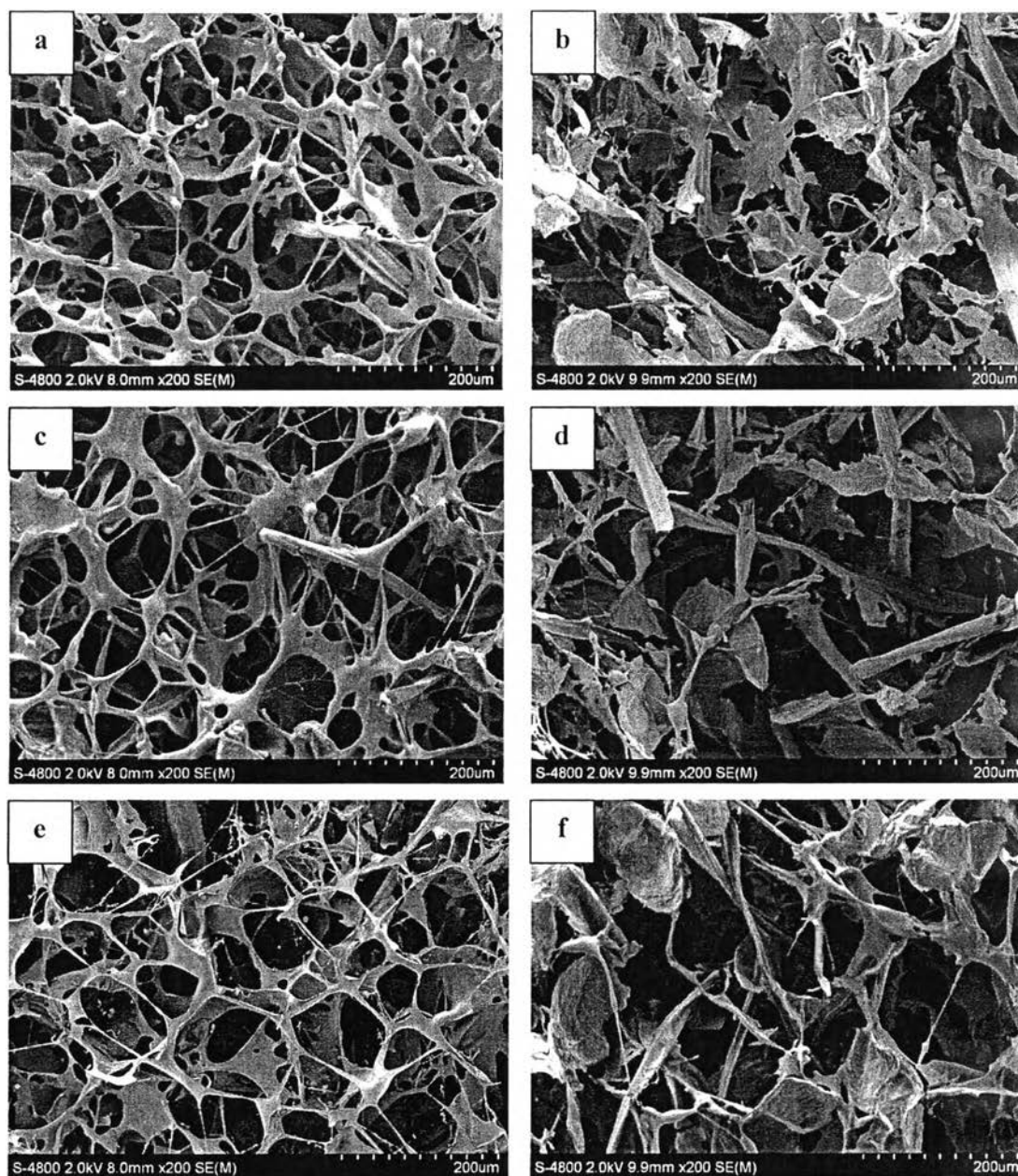
Figure 4.6 SEM images of top surface of (a), (c) and (e) bionanocomposite sponges at SF/CLWs ratio of 70/30, 60/40 and 50/50 respectively. (b), (c) and (f) represented cross sectional part of bionanocomposite sponges at SF/CLWs ratio of 70/30, 60/40 and 50/50 respectively.

4.4.5.2 Chemical Analysis of Bionanocomposite Sponges

From figure 4.7 (a) the FTIR spectra, the characteristic peaks of the neat SF locating at 1654 cm^{-1} (amide I) and 1542 cm^{-1} (amide II) which are attributed to a random coil structure or silk I (Yang *et al.*, 2000; Noshiki *et al.*, 2002; Freddi *et al.*, 2003; Park *et al.*, 2004). On the contrary, the FTIR spectra of the biocomposite sponges with the increasing of CLWs content show a gradual shift of those characteristics peaks of silk I to 1630 cm^{-1} (amide I) and 1523cm^{-1} (amide II), implying the conformation transition from random coil conformation to β-sheet structure of the SF matrix. The highest intensities of the characteristic peaks of beta-sheet structure in the FTIR spectra is observed at the SF/CLWs ratio of 50/50. Nevertheless, the FTIR spectra of all biocomposite shows the characteristic peaks of CLWs at 1167 cm^{-1} and 1060 cm^{-1}, corresponding to the C-O-C asymmetric stretching and the C-O symmetric stretching in the CL structure (Barud *et al.*, 2008). The conversion of SF structure from random coil into β-sheet should be enhanced by blending the SF with the CLWs because the surface of crystalline CLWs and the interactions, like hydrogen bonding, between – OH of CLWs and –NH$_2$ and/or –OH group in SF induces the transition of SF conformation during the fabrication of composite sponges. A similar conformational transition was also found in the blended membrane of CL and SF (Noshiki *et al.*, 2002) the SF/microcrystalline CL film (Park *et al.*, 2004) and the electrospun nanofibers of chitosan containing SF (Barud *et al.*, 2008).

There are many methods to induce conformation transition such as thermal, mechanical or chemical treatments but the most common and widely used method is methanol treatment. The immersion in polar solvent, particularly aqueous methanol, are highly effective in cystallization of SF (Park *et al.*, 2004). Thus, after treated with methanol, all bionanocomposite sponges exhibited β-sheet conformation at to 1630 cm^{-1} (amide I) and 1523cm^{-1} (amide II) as shown in Figure 4.7 (b). The peaks were shifted after methanol treatment due to the methanol molecule able to interferes the hydrogen bond of random coil SF and induce the beta-sheet conformation.
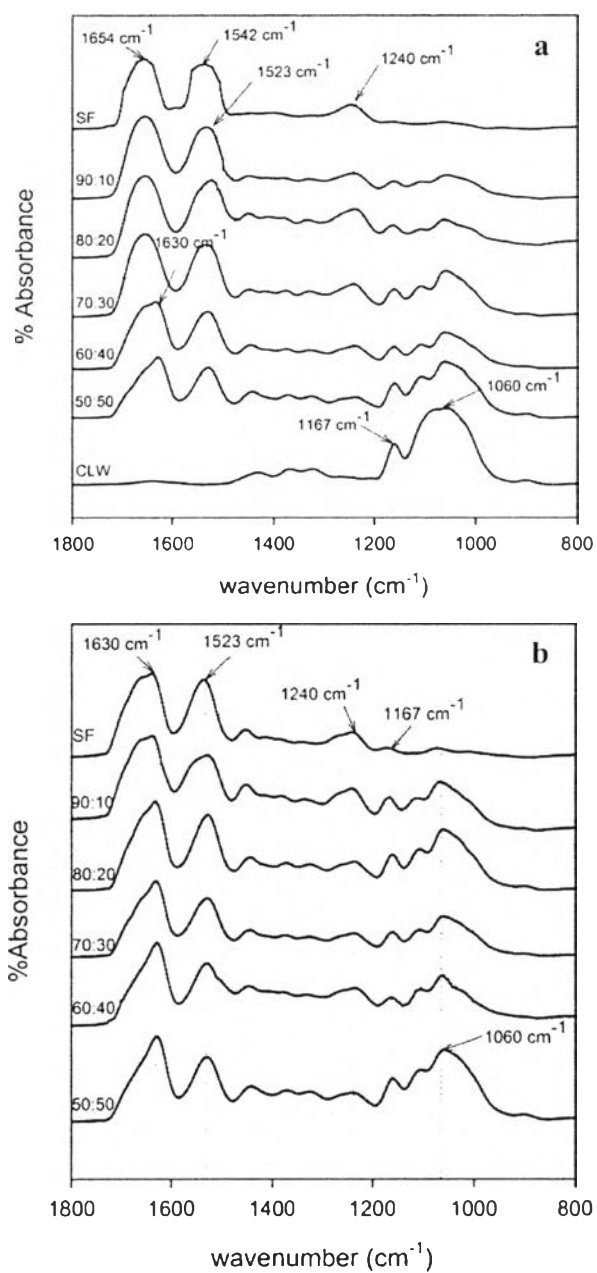
Figure 4.7 FTIR spectra of SF, CLWs, and SF/CLWs bionanocomposite sponges (a) before and (b) after methanol treatment.

4.4.5.3 Weight Loss of Non-methanol Treated and Methanol Treated Bionanocomposite Sponges

From figure 4.8, the weight loss (%) of the non-methanol treated bionanocomposite sponges increased with increasing immersion time. However, it is obviously seen that the incorperation of CLWs could reduce the weight loss of the bionanocomposite sponges. Moreover, the weight loss of methanol-treated bionanocomposite sponges were significantly decreased which more stable in water than the non-treated ones. The better dimension stability in water of the bionanocomposite sponges resulted from the conformation transition from random coil to beta-sheet structure, the water stable conformation, which in the same way of FTIR results that showed the characteristic peaks of beta-sheet conformation. However, the methonol treatment gave a larger effect on conformation transition than the incorporation CLWs in SF matrix. The methanol treated bionanocomposite sponge at SF/CLWs ratio of 50/50 possed more excellent water stabilitity in this study.
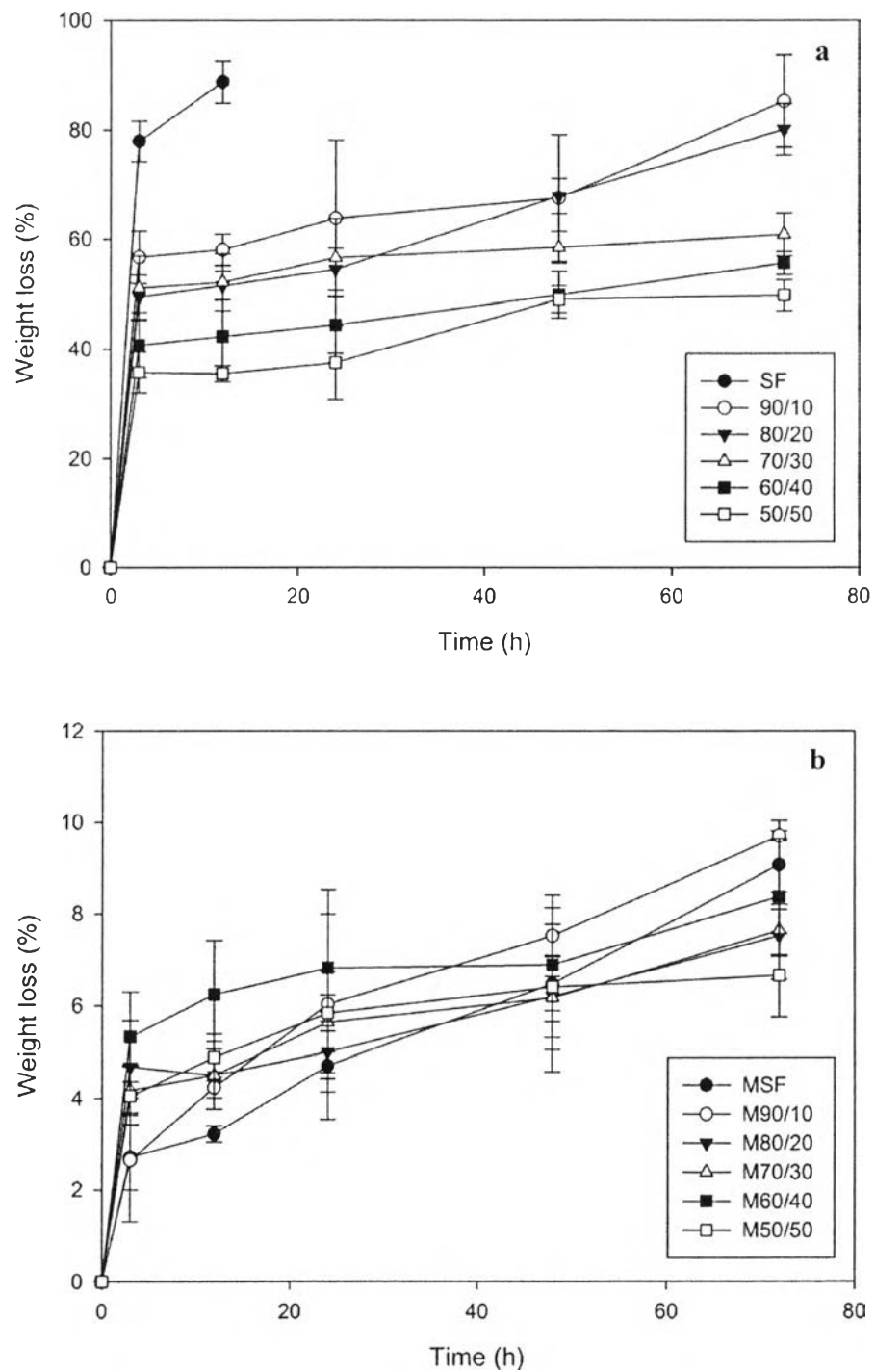
Figure 4.8 Weight loss of (a) non-methanol treated and (b) methanol treated bionanocomposite sponges.

4.4.5.3 Dimensional Stability and Compression Modulus of Methanol Treated Bionanocomposite Sponges

The change of volume of the bionanocomposite sponges before and after methanol treatment was measured in order to determine dimensional stability of the bionanocomposite sponges. In general, the transition induction effects to the shrinkage of material, especially the porous material, resulted to poor dimensional stability. As shown in Figure 4.9, the shrinkage (%) of the neat silk fibroin sponges owned the highest shrinkage. The incoperation of CLWs in any weight ratios could reduced the shirkage (%) of bionanocomposite sponges after treated with methanol. The compression modulus of the CLWs-reinforced SF sponges were remakable higher than the neat SF sponges and began to level off at approximately 235 to 249 kPa at 40 and 50% of CLWs as shown in Figure 4.10. These results may assign to the β-sheet conformation of SF when incorperated with 50% CLWs which caused by the inter-molecular hydrogen bond between amide group of SF and hydroxyl group of CLWs, as shown in figure 4.11, that drived the formation of β-sheet conformation and promoted the crystallinity resulting to possed higher modulus. This phenomenon also correspond to the result reported by Noshiki *et al.* (2001) which prepared silk fibroin-microcrystalline cellulose (cellulose whiskers) by casting mixed aqueous solution. The Young's modulus of the composite films was dependence on mixing ratio which reached its maximum at 70-80% cellulose content, five times of pure fibroin or pure cellulose film. Marsano *et al.* (2008) evaluated the regenerated cellulose – fibroin blends fiber. They found the fiber that contained 75% cellulose showed better mechanical properties than pure cellulose which indicated the good interation and a good compatibiliy.
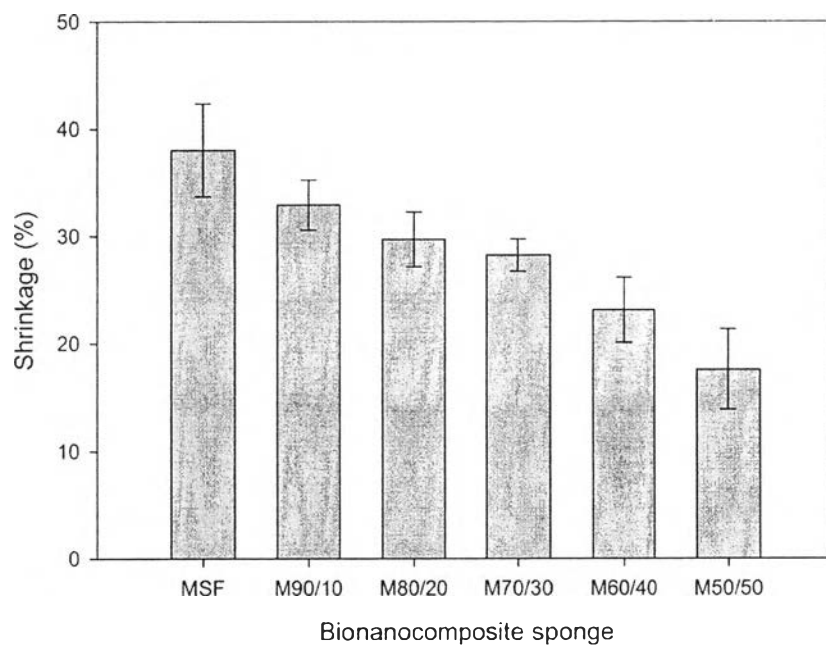
Figure 4.9 Shrinkage (%) of bionanocomposite sponges after methanol treatment.
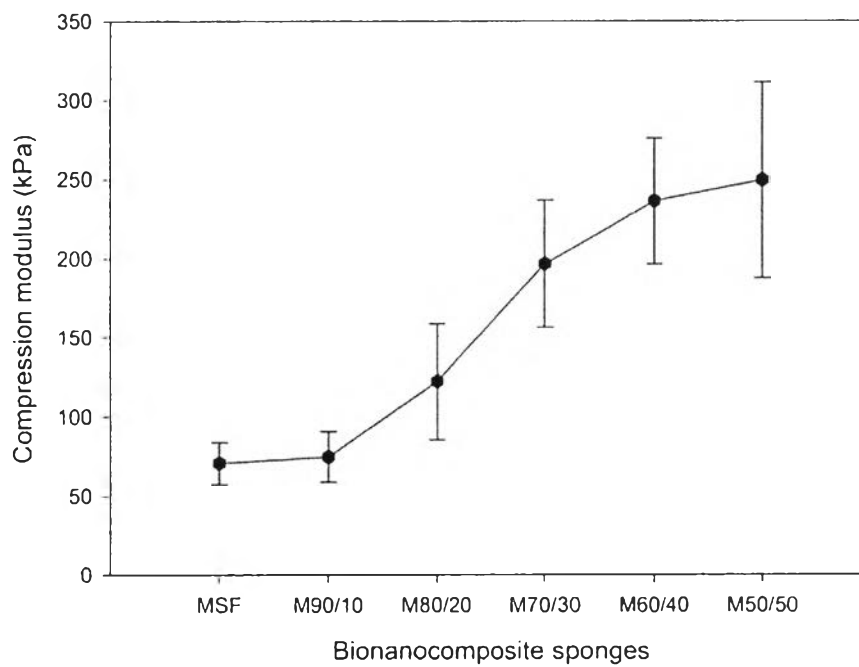

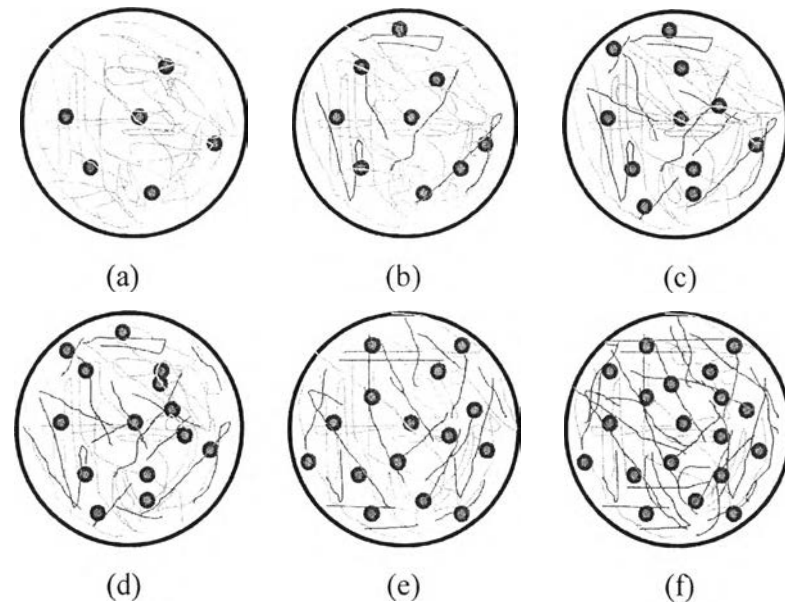**Figure 4.10** Compression modulus of methanol- treated bionanocompostie sponges

Figure 4.11 Schematic model proposed for hydrogen bonding in SF/CLWs bionanocomposite sponge (a), (b), (c), (d), (e), and (f) represented bionanocomposite sponge at weight ratio of SF/CLWs 100/0, 90/10, 80/20, 70/30, 60/40 and 50/50 respectively (........ SF, ▬▬ CLWs, o hydrogen bond).

4.4.6 Yeast Cell Immobilization and Cell Leakage

Figure 4.12 represented FE-SEM images of a large number of yeast cell attached inside bionanocomposite sponges at 50/50 of SF/CLWs weight ratios. Direct count of yeast cell by using Neubaeur Precicolor HBG heamacytometer counting chamber was used to reveal the number of yeast cell. The bionanocomposite sponges at SF/CLWs ratio of 50/50 had the highest number of cell attached inside which may resulted from the largest pore sizes that allowed better yeast cell penetration and nutrient transfer during immobilization step compared to the smaller. Moreover, the CLWs exhibited long and slender fiber which provided high surface area for yeast attachment. Thus, the high surface area for yeast to attach was provided at 50/50 weight ratio of SF/CLWs bionanocomposite sponge.

Another factor is the adhesion properties of yeast cell that able to adapt to new environments by specialized protein on cell surface called "adhesin" (Verstrepen and Klis., 2006; Rapoport *et al.*, 2011). It was reported that in unfavorable conditions, cell will reduce its size, lowered metabolism and increased adhesiveness in order to survive (Characklis *et al.*, 1990) which enhanced the immobilization. The cell preferred to attach on solid surface which provided the protection and available nutrient (Schott *et al.*, 1995). In this experiment, after immobilization, the yeast cell in bionanocomposite sponges was freeze-dried together which reduced the moisture content in cell biomass which stressed yeast cells. Bekers *et al.*, 1999 reported that dehydration of yeast cell destroyed some cell wall structure and the extracellular polymer substance leaked out from cell wall and form biofilm which further the immobilization (Bekers *et al.*, 1981; Flemming *et al.*, 1998). Unfortunately, the adhesion of yeast cells did not lead to stable immobilization, so some amount of yeast cell leaked after rehydrated the bionanocomposite in fermentation step. The bionanocomposite sponges at SF/CLWs ratio of 50/50 showed the highest yeast cell immobilization (%) after revitalization.
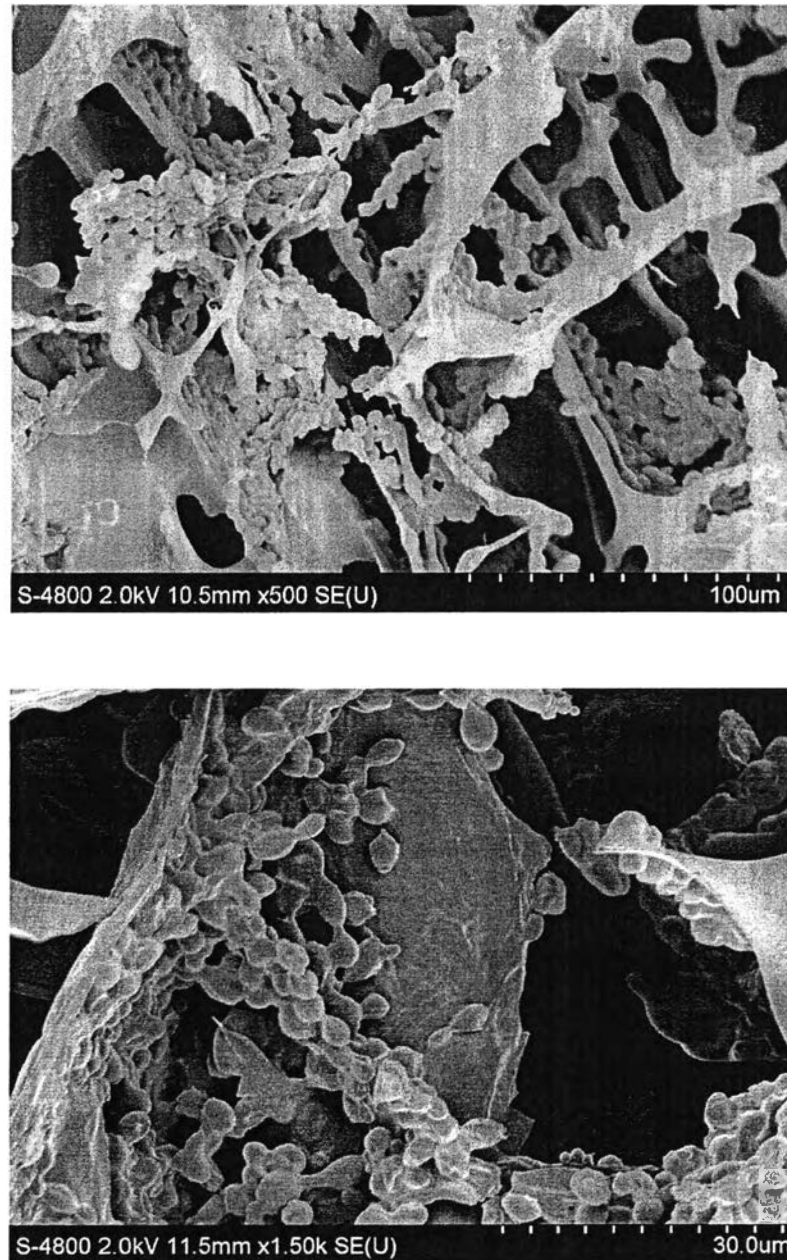
Figure 4.12 Field Emission Scanning Electron micrographs of bionanocomposite sponge having SF/CLWs weight ratio of 50/50 after immobilization of yeast cells.
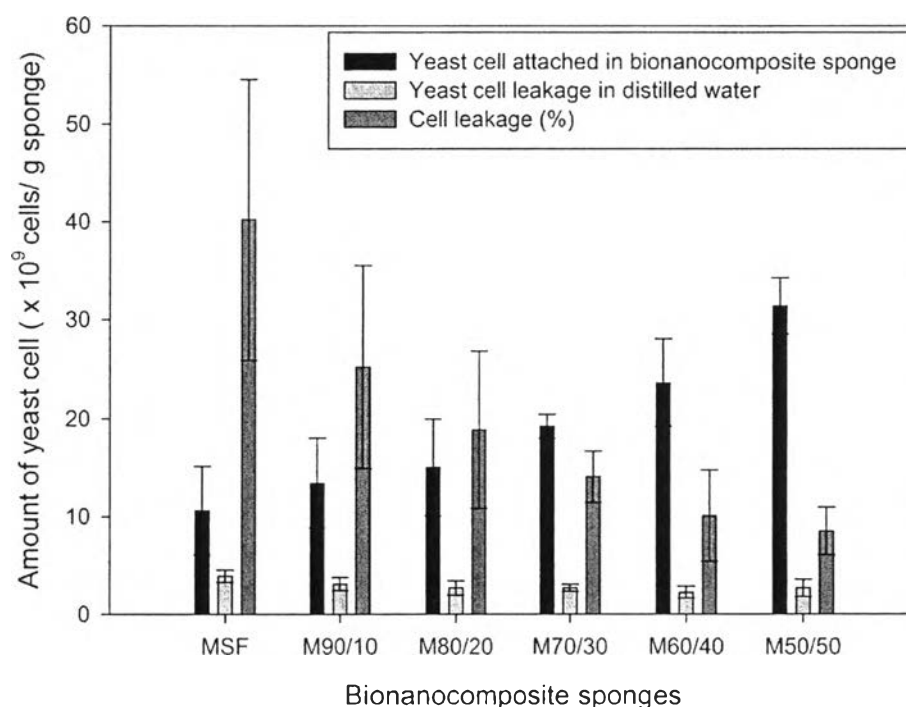
Figure 4.13 Yeast cell leakage in distilled water after immersed in distilled water for 48 hour under fermentation condition.

4.4.7 Properties of Immobilized Yeast Cells With and Without Glyoxal Crosslinked for Ethanol Production

4.4.7.1 Comparison of Immobilization Efficiency between Immobilized Yeast Cell With and Without Glyoxal Crosslinked in Bionanocomposite sponges

Ethanol production by using yeast cell immobilization in bionanocomposite sponges at SF/CLWs ratio of 50/50 was further examined by batch fermentation. Glucose solution with varied concentration, 10%, 20%, 30% and 40% (w/v), was used as a substrate. To enhance the immobilization efficiency, the immobilized cells were crosslinked by immersed the bionanocomposite sponge containing yeast cell in 0.01 mM glyoxal solution for 24 hours then immersed in 0.1 M glycine solution to get rid of the excess glyoxal.

The immobilization efficiency was calculated by counting yeast cell concentration both inside the bionanocomposite sponge and suspended yeast cells in glucose solution after batch fermentation. It was found that at any concentration of glucose, the immobilization efficiency was enhanced with glyoxal crosslinked which higher than the immobilized cell without crosslinked at between 10-20% as shown in Figure 4.14. The glyoxal crosslinked was expected to crosslink glycoprotein, the combination of mannose sugar and protein which exists about 40% of outer part of yeast's cell wall (Klis *et al.,* 2006) with hydroxyl (-OH) group of CLWs or serine protein in SF.
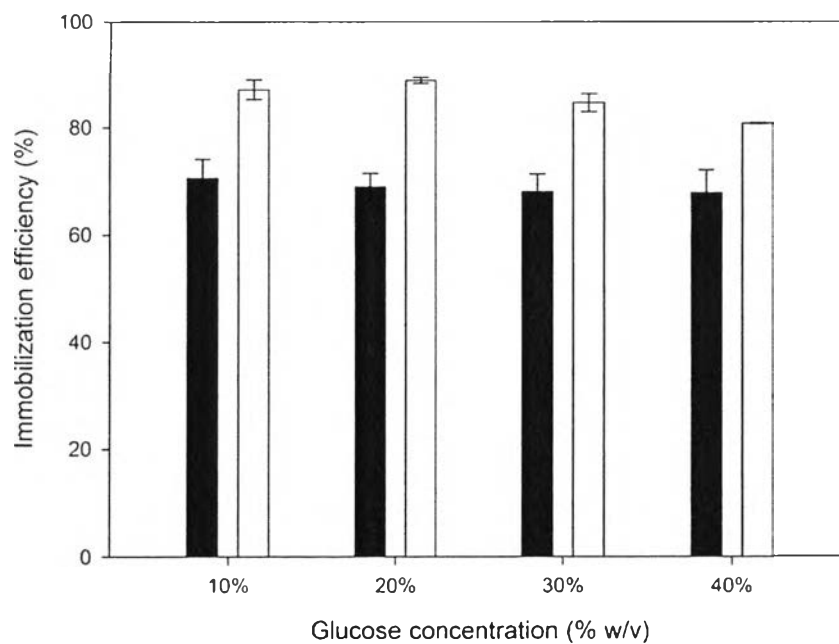

Figure 4.14 Immobilization efficiency (%) of immobilized cell (▇)and immobilized cell with glyoxal crosslinked (▭) at various glucose concentration.

Table 4.5 Macromolecules of cell wall of *S. cerevisiae* (Klis *et al.*, 2006)

Macromolecule	% of wall mass
Mannoproteins	30-50
1,6-β-Glucan	5-10
1,3-β-Glucan	30-45
Chitin	1.5-6

4.4.7.2 Investigation of the Effect of Sugar Concentration on Ethanol Production from Batch Fermentation System of Free Yeast Cell, Immobilized Yeast Cell With and Without Glyoxal Crosslinked

The immobilized yeast cell with and without crosslinked and free cell were inoculated into three 250 ml flasks with 100 ml of fermentation medium and sampling from each fermentation system at specific time intervals. The ethanol production and glucose consumption were compared between three systems. Table 4.6 - 4.9 summarized glucose consumption (Y_s), ethanol production (Y_p), and ethanol yield over substrate ($Y_{p/s}$) at each glucose concentration. Maximum ethanol production was 30.25 g/l at 20% glucose, 45.32 g/l at 30% glucose and 37.12 g/l at 30% glucose for free cell, immobilized cell and glyoxal crosslinked immobilized cell fermentation system, respectively.

Table 4.6 The immobilized efficiency, glucose consumption (Y_s), ethanol production (Y_p), ethanol yield ($Y_{p/s}$) in ethanol production used 10% (w/v) glucose as substrate.

System	Cell concentration (x 10^9 cell)			Immobili-zation efficiency (%)	Sugar consumption ($Y_s = S_0-S$) (g/l)	Ethanol ($P-P_0$) (g/l)	$Y_{P/S}$
	X_f	X_i	X_t				
Free cell	4.1	-	4.10	-	83.84	20.42	0.24
Immobilized cell	1.92	4.62	6.54	70.55	90.84	21.78	0.24
crosslinked cell	0.883	6.03	6.92	87.14	78.30	20.68	0.26

Table 4.7 The immobilized efficiency, glucose consumption (Y_s), ethanol production (Y_p), ethanol yield ($Y_{p/s}$) in ethanol production used 20% (w/v) glucose as substrate.

System	Cell concentration (x 10^9 cell)			Immobili-zation efficiency (%)	Sugar consumption ($Y_s = S_0-S$) (g/l)	Ethanol ($P-P_0$) (g/l)	$Y_{P/S}$
	X_f	X_i	X_t				
Free cell	4.55	-	4.55	-	142.71	30.25	0.21
Immobilized cell	2.37	5.28	7.65	68.93	166.15	39.17	0.24
crosslinked cell	1.01	9.07	10.10	89.87	154.43	33.71	0.22

Table 4.8 The immobilized efficiency, glucose consumption (Y_s), ethanol production (Y_p), ethanol yield ($Y_{p/s}$) in ethanol production used 30% (w/v) glucose as substrate.

System	Cell concentration (x 10^9 cell)			Immobili-zation efficiency (%)	Sugar consumption ($Y_s = S_0$-S) (g/l)	Ethanol (P-P_0) (g/l)	$Y_{P/S}$
	X_f	X_i	X_t				
Free cell	3.75	-	3.75	-	171.76	22.83	0.13
Immobilized cell	2.03	4.34	6.37	67.97	233.05	45.32	0.19
crosslinked cell	1.33	7.37	8.69	84.65	211.57	37.12	0.18

Table 4.9 The immobilized efficiency, glucose consumption (Y_s), ethanol production (Y_p), ethanol yield ($Y_{p/s}$) in ethanol production used 30% (w/v) glucose as substrate.

System	Cell concentration (x 10^9 cell)			Immobili-zation efficiency (%)	Sugar consumption ($Y_s = S_0$-S) (g/l)	Ethanol (P-P_0) (g/l)	$Y_{P/S}$
	X_f	X_i	X_t				
Free cell	3.58	-	3.58	-	185.77	24.26	0.13
Immobilized cell	1.92	4.08	6.00	67.77	216.46	42.49	0.20
crosslinked cell	2.01	6.43	8.44	76.19	199.49	35.94	0.18

According to figure 4.15, the ethanol production by free yeast cell fermentation system was significantly dropped when using glucose concentration higher than 20% (w/v) as a substrate which due to substrate inhibition. In industrial, the yeast activities normally have limited osmotolerance which often caused by the substrate and product inhibition (Phisalaphong *et al.,* 2005). The free yeast cell directly exposed

to high concentration of substrate which caused the concentration gradient between water in yeast cell and outer environment. The water in yeast cell diffused out through its cell membrane leading to cell plasmolysis and cell death. This phenomemon called "substrate inhibition" that caused low ethanol production when high concentration of substrate was applied. As shown in figure 4.16, the viable yeast cell at the end of fermentation by using free yeast cell system was the lowest among three systems due to some yeast cells were plasmolysed. For immobilized yeast cell in bionanocomposite sponge, which acting as protector and holding high cell concentration compared to the free one which exposed to the highly substrate inhibition. Moreover, immobilization provides favorable microenvironment conditions, cell-cell contact and nutrient-product gradients, resulting to better performance in ethanol fermentation. It was found that, at high sugar concentrations, the fermentation system using bionanocomposite immobilized yeast cell was more efficient than when using free cells. Although glyoxal crosslinking able to enhance immobilization efficiency but the existence of chemical bond of glyoxal crosslinking effected to the yeast cell activity resulting to lower bioethanol production.
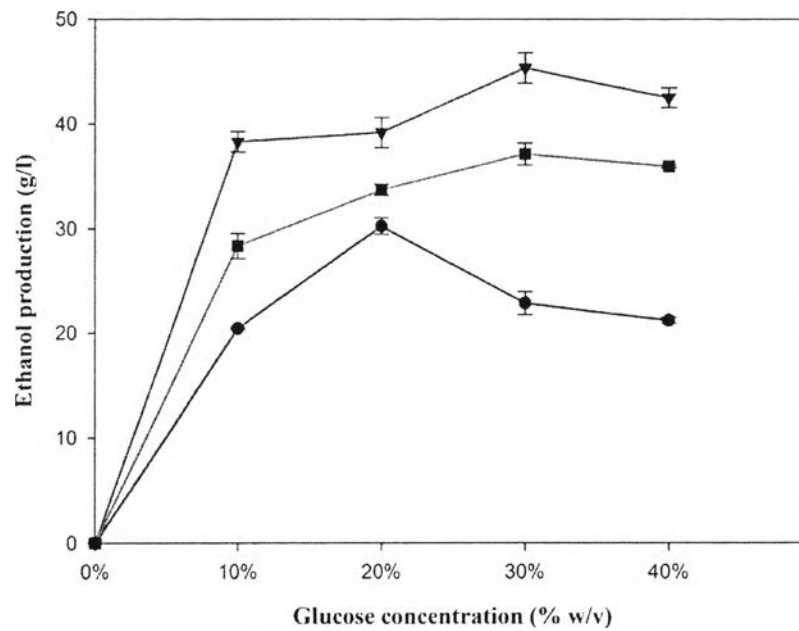
Figure 4.15 Ethanol production at varied glucose concentration —•— free yeast cell, —▼— immobilized yeast cell and —■— glyoxal crosslinked yeast cell system.
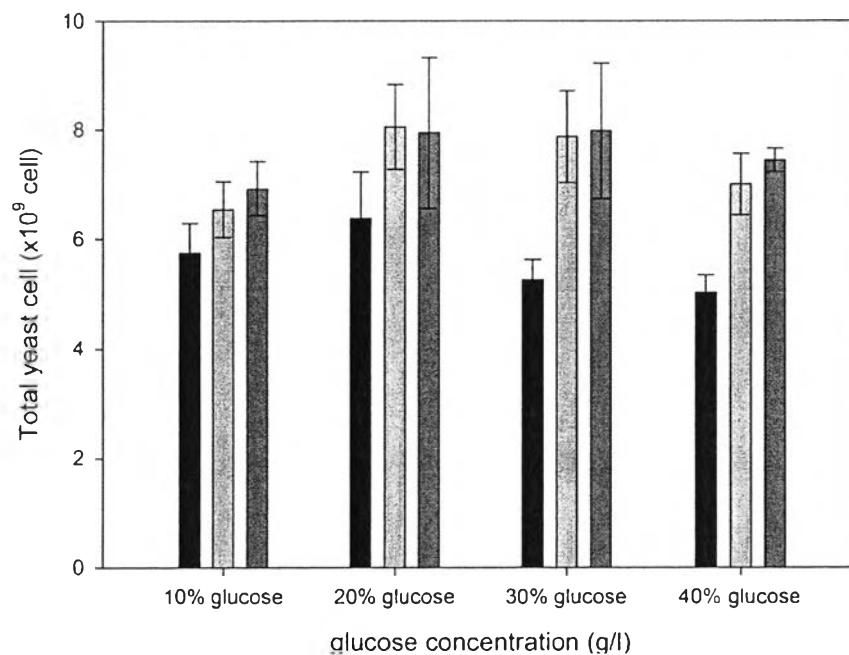

Figure 4.16 Viable yeast cells at the end of fermentation in varied glucose concentration ■ free yeast cell, ▱ immobilized yeast cell and ▨ immobilized yeast cell with crosslinking.

Another factor that used to evaluate the potential of ethanol fermentation is the conversion of glucose into ethanol. The conversion (%) of each fermentation system was shown in table 4.9. In theoretically, 1 g of glucose will be converted by enzyme from yeast cell during fermentation into a product, ethanol, 0.51 g and 0.49 g of carbon dioxide (CO_2) as by-product (Shuler and Kargi, 2002) as shown in equation 4.9. However, in this study, the maximum conversion of glucose into ethanol was about 26.41% which lower than the theoretical yield 24.59%. This might resulted from the ineffective control during fermentation that allowed oxygen pass through the system which should be anaerobe. According to equation 4.10, in aerobic condition, the fermentation is not completely take place due to yeast cells prefer to use glucose, a carbon source, in their respiration pathway to obtain ATP energy that use in cell activity and increase amount of cell instead of use in fermentation (Shuler and Kargi, 2002). In addition, the culture medium also affect to cell activities. In this experiment, only glucose which is a carbon source was applied in the fermentation. The medium should consist of carbon source, nitrogen source, trace elements and vitamins required to enhance cell metabolisms resulting to better yield in ethanol fermentation.

Table 4.10 The conversion of glucose into ethanol (%)

Fermentation system	Free cell	Immobilized cell	Immobilized cell with glyoxal crosslinked
10% glucose	24.36	23.98	26.41
20% glucose	21.20	23.58	21.83
30% glucose	13.29	19.45	17.55
40% glucose	13.06	19.63	18.02

Equation 4.9 Alcoholic fermentation by yeast under anaerobic condition

$$C_6H_{12}O_6 \longrightarrow C_2H_5OH + 2CO_2 + Energy$$

100%   51%   49%
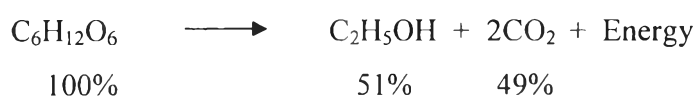
Equation 4.10 Fermentation under aerobic condition

$$C_6H_{12}O_6 + 6O_2 \longrightarrow 6CO_2 + 6H_2O + Energy$$

4.4.7 Repeat Batch Fermentation by Using Yeast Cell Immobilized in Bionanocomposite Sponge

Ethanol production using yeast cell immobilized in 50/50 ratio of SF/CLWs bionanocomposite sponge was further evaluated by five-cycle repeated batch fermentation. The solution composed of glucose 400 gl^{-1}, peptone 20 gl^{-1} and yeast extract 10 gl^{-1} was used as a substrate. The ethanol production ($Y_{p/s}$) and glucose consumption (Y_s) was compared with free cell system. The duration of each batch was set at 48 hours. After reached the end of fermentation time, the bionanocomposite sponges were transferred into a newly prepared substrate and started the next batch. Table 4.10 summarizes sugar consumption, ethanol production, ethanol yield (Yp/s) and conversion of glucose into ethanol (%) of five repeated batch. The free cell fermentation was done in order to compare the efficiency of cell immobilization. In the first to third batches, the immobilized yeast cell system provided higher ethanol production (g/l) than free cell fermentation about 28%, 65% and 54%, respectively. The ethanol production was significantly increased after the first batch which resulted from the larger amount of yeast cell that has been grown during 48 hours of the first batch. As mentioned earlier, the substrate and product inhibition are normally observed. The bionanocomposite sponge provided a protection to the yeast cell against high concentration of glucose, which caused the plasmolysis of cell, and the toxicity of ethanol. Thus, the immobilization lessen the affect of inhibition which leading to cell death and also maintained the production capacity in repeat batch system as shown in figure 4.17. The ethanol production was increased after the first batch and tended to decrease after the fifth batch. However, the conversion of glucose into ethanol (%) was still maintained which suggested that the activity of yeast cell was not change during the repeated batch but it may need longer fermentation time to obtain high ethanol production.

Table 4.11 The sugar consumption (Y_s), ethanol production (P), ethanol yield ($Y_{p/s}$) and conversion of glucose into ethanol of five repeated batches fermentation by using free cell and immobilized cell.

| Batch number	System	Sugar consumption ($Y_s = S_0-S$) (g/l)	Ethanol ($P-P_0$) (g/l)	$Y_{P/S}$	Conversion of glucose into ethanol (%)
1	Free cell	313.09	63.40	0.20	20.24
	Immobilized cell	303.28	81.39	0.29	26.84
2	Free cell	263.66	63.74	0.24	24.17
	Immobilized cell	315.79	105.21	0.33	33.32
3	Free cell	259.42	66.96	0.26	25.81
	Immobilized cell	309.05	103.19	0.33	33.39
4	Immobilized cell	288.24	100.54	0.35	34.83
5	Immobilized cell	286.40	91.83	0.32	31.82
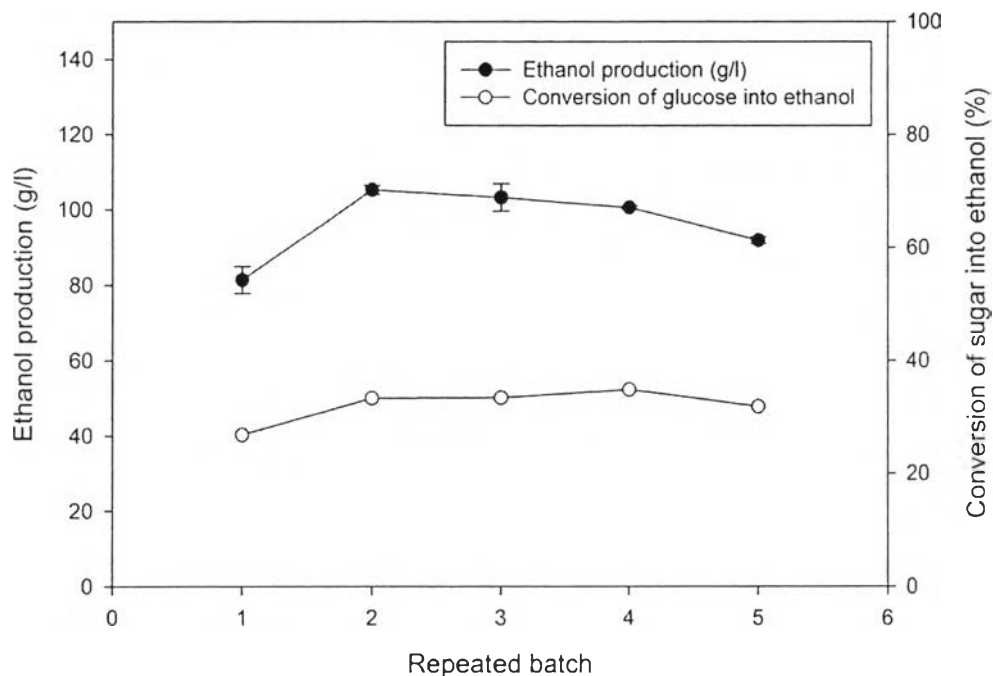
Figure 4.17 Ethanol production (g/l) and conversion of glucose into ethanol (%) during five- cycle repeated batches.

4.5 Conclusions

In this work, a bionanocomposite sponges of SF and CLWs were fabricated by freeze drying technique by varying the blend ratios of SF and CLWs. The obtained bionanocomposite sponges had interconnected porous structure. The conversion of SF conformation from random coil into β-sheet should be enhanced by blending the SF with the CLWs because the interactions, like hydrogen bonding, between SF and CLWs induce the transition of SF conformation. The methanol treatment also able to enhance the conformation transition which significantly increase the water stability of the sponges. The SF/CLWs bionanocomposite sponges could be used as a supporting matrix for immobilization of yeast cell for using in ethanol production. The immobilization of *S. cerevisiae burgundy* KY11 was performed by adsorption of the yeast cells on SF/CLWs sponges. The 50/50 ratio of SF/CLWs bionanocomposite was chosen as a

matrix due to its large pore width that allowed the largest amount of yeast cell pass through and the CLWs exhibited long and slender fibril that provided high surface area for yeast attachment. The fermentation was performed by using glucose with varied concentration as a substrate. The system using immobilized yeast cells were more efficient than when using free cells based on glucose conversion into ethanol (%). Immobilization can lessen the effect of substrate inhibition. The glyoxal crosslinked improved cell immobilization efficiency but its toxicity affected to cell's activities. The yeast immobilized bionanocomposite sponges able to be reuse with stability yield. In addition, after the end of fermentation, the bionanocomposite sponge containing yeast cell can be used as animal feed due to SF and yeast cell are excellent sources of protein and also biodegradable.

ACKNOWLEDGEMENT

REFERENCES

Altman, G.H., Diaz, F., Jakuba, T., Calabro, R.L., Chen, J. and Kaplan, D. (2003) Silk-based biomatetails, bioethenol. Biomaterial, 25, 401-416.

Aggarwal, N.K., Nigam, P., Yadav, B.S. and Singh, D. (2001). Process for the production of sugar for bioethanol industry from sorghum a non-conventional source of starch. World J Microbial Biotechnol, 17, 125-131.

Chen, X., Li, W., and Yu, T. (1997) Conformation transition of silk fibroin induced by blending chitosan. Polymer Science, 35, 2293-2296.

Chen, J.Y., Wu, K.W. and Fukuda, H. (2008). Bioethanol production from cookies raw starch by immobilized surface-engineered yeast cells. Applied Biochem Biotechnol, 145, 59-67.

Cunha, M.A.A., Rodrigues, R.C.B., Santos, J.S., Conveti, A. and da Silva, S.S. (2007). Repeated batch xylitol bioproduction using yeast cells entrapped in polyvinyl alcohol hydrogel. Current Microbiology, 54, 91-96.

Demeny, Z., Smogrovocova, D., Gemeiner, P., Malovikova, A., and Strudik, E. (1996) Calcium pectate gel to immobilize yeast for continuous beer production, Proc. Int. Workshop Bioencapsulation, 12, 1-4.

Domeny, Z., Smogrovicova, D., Gemeiner, P., Sturdik, E., Patkova, J. and Malovikova, A. (1998). Continuous secondary fermentation using immobilized yeast. Biotechnology Letters, 11, 1041-1045.

Elanthikkal, S., Gopalakrishnapanicker, U., Varghese, S., and Guthrie, J.T. (2010). Cellulose microfibers produced from banana plant wastes: Isolation and characterization. Carbohydrate Polymers, 80, 852-859.

Freddi, F., Romano, M., Massafra, M.R., and Tsukuda, M. (1995) Silk fibroin/cellulose blend films: Preparation, structure and physical properties. Applied Polymer Sciece, 56, 1537-1545.

Gosline, J.M., Guerette, P.A., Ortlepp, C.S., and Savage, K.N. (1999) The mechanical design of spider silks: from fibroin sequence to mechanical function. Experimental Biology, 23, 3295-3303.

Hakimi, O., Knight, D.P., Vollrath, F., and Vadgama, P. (2007) Spider and mulberry silkworm silks as compatible biomaterials. Composites part B, 38, 324- 337.

He, S.J., Valluzzi, R.,and Gido, S.P. (1999) Silk I structure in Bombyx mori silk foams. International Journal of Biological Macromolecules, 24, 187-195.

Kongdee, A., Bechtold, T., and Teufel, L. (2004). Modification of cellulose fiber with silk sericin. Applied Polymer Science, 96, 1421-1428.

Kumakura, M., Yoshida, M., and Asano, M. (1992). Preparation of immobilized yeast cells with porous substrates. Process Biochemistry, 27, 225-229.

Liang, C.X., Hirabayashi, K. (1992) Improvement of the physicalproperties of fibroin membrenes with sodium alginate, Applied Polymer Science, 45, 1937-1943.

Liu, R., and Shen, F. (2008). Impact of main factors of bioethanol fermentation from stalk juice of sweet sorghum by immobilized *Saccharomyces cerevisae* (CICC 1308). Bioresource Technology, 99, 847-854.

Nedovic, V., Obradovic, B., Vunjak-Novakovic, G., and Leskosek-Cukalovic, I. (1993) Kinetics of beer fermentation with immobilized yeast cells in an internal loop air-lift bioreactor. Hem. Ind. (in Serbian), 47, 168-172.

Nigam, J.N., Gogoi, B.K., and Bezbarauh, R.L. (1998). Short communication: Alcoholic fermentation by agar-immobilized yeast cells. World Journal of Microbiology and Biotechnology, 14, 457-459.

Nigam, S.P., and Singh, A. (2011) Production of liquid biofuels from renewable resources. Progress in Energy and Combustion Science, 37, 52-68.

Onaka, T., Nakanishi, K., Inoue, T. and Kubo, S. (1985) Beer brewing with immobilised yeast. Bio/Technology, 3, 467- 470.

Phisalaphong, M., Srirattana, N., and Tanthapanichakoon, W. (2005) Mathematical modeling to investigate temperature effect on kinetic parameters of ethanol fermentation, Biochemical Engineering Journal 28, 36–43.

Plessas, S., Bekatorou, A., Koutinas, A.A., Soupioni, M., Banat, I.M., and Marchant, R. (2007). Use of *Saccharomyces cerevisae* cells immobilized on orange peel as biocatalyst for alcoholic fermentation. Bioresource Technology, 98, 860-865.

Rakin, M., Mojovic, L., Nikolic, S., Vukasinovic, M., and Nedovic, V. (2008). Bioethanol production by immobilized *Saccharomyces cerevisae* var. ellipsoideus cells. African journal of Biotechnology, 8(3), 464-471.

Razmovski, R., and Vucurovic, V. (2011). Ethanol production from sugar beet molasses by *S. cerevisiae* entrapped in an alginate-maize stem ground tissue matrix. Enzyme and microbial technology.

Rodriguez, N.L.G., Thielemans, W., and Dufresne A. (2006). Sisal cellulose whiskers reinforced polyvinyl acetate nanocomposite. Cellulose, 13, 261-270.

Samir, M.A.S.A., Alloin, F., and Dufresne, A. (2005). Review of recent research into cellulosic whiskers, their properties and their application in nanocomposite field. Biomacromolecules, 6, 612-626.

Siqueira, G., Bras, J., and Dufresne, A. (2009). Cellulose whiskers versus microfibrils: Influence of the nature of the nanoparticle and its surface functionalization on the thermal and mechanical properties of nanocomposites. Biomacromolecules, 10, 425-432.

Verma, G., Nigam, P. Singh, D. and Chaudhary, K. (2000) Bioconversion of starch to ethanol in a single-step process by co-culture of amylolytic yeasts and *Saccharomyces cerevisiae 21*. Bioresour Technol, 72, 261-266.

White, F.H., and Portno, A.D. (1978) Continuous fermentation by immobilized brewer yeast. Journal of the Institute of Brewing&Distilling, 84, 228- 230.

Winkelhausen, E., Velickova, E., Amartey, S.A., and Kuzmanova, S. (2010). Ethanol production using immobilized *Saccharomyces cerevisae* in lyophilized cellulose gel. Applied Biochem Biotechnology, 162, 2214-2220.

Wongpanit, P., Sanchavanakit, N., Pavasant, P., Bunaprasert, T., Tabata, Y., and Rujiravanit, R. (2007). Preparation and characterization of chitin whisker-reinforced silk fibroin nanocomposite sponges. European Polymer Journal, 43, 4123-4135.

Wu, J.H., Wang, Z., and Xu, S.Y. (2007). Preparation and characterization of sericin powder extracted from silk industry waste water. Food Chemistry, 103, 1255-1262.

Zhang, Y.Q. (2002). Applications of natural silk protein sericin in biomaterial. Biotechnology Advances, 20, 91-100

Zuluaga, R., Putaux, J.L., Cruz, J., Velez, J., Mondrago, I., and Ganan, P. (2009). Cellulose microfibrils from banana rachis: Effect of alkaline treatments on structural and morphological features. Carbohydrate Polymers, 76, 51-59.

Zuluaga, R., Putaux, J.L., Restrepo, A., Mondragon, I., and Gañán, P. (2007). Cellulose microfibrils from banana farming residues: isolation and characterization. Cellulose, 14(6), 585-592.